

The Schizophrenic Spectrum of LSR 1610–0040: a Peculiar M Dwarf/Subdwarf

Michael C. Cushing^{1,2}

Steward Observatory, University of Arizona, 933 North Cherry Avenue, Tucson, AZ 85721

mcushing@as.arizona.edu

and

William D. Vacca¹

SOFIA-USRA, NASA Ames Research Center MS N211-3, Moffett Field, CA 94035

wvacca@mail.arc.nasa.gov

ABSTRACT

We present a moderate resolution ($R \equiv \lambda/\Delta\lambda \approx 2000$), 0.8–4.1 μm spectrum of LSR 1610–0040, a high proper motion star classified as an early-type L subdwarf by Lépine and collaborators based on its red-optical spectrum. The near-infrared spectrum of LSR 1610–0040 does not fit into the (tentative) M/L subdwarf sequence but rather exhibits a mix of characteristics found in the spectra of both M dwarfs and M subdwarfs. In particular, the near-infrared spectrum exhibits a Na I doublet and CO overtone bandheads in the K band, and Al I and K I lines and an FeH bandhead in the H band, all of which have strengths more typical of field M dwarfs. Furthermore the spectrum of Gl 406 (M6 V) provides a reasonably good match to the 0.6–4.1 μm spectral energy distribution of LSR 1610. Nevertheless the near-infrared spectrum of LSR 1610 also exhibits features common to the spectra of M subdwarfs including a strong Ti I multiplet centered at $\sim 0.97 \mu\text{m}$, a weak VO band at $\sim 1.06 \mu\text{m}$, and possible collision-induced H₂ absorption in the H and K bands. We discuss a number of possible explanations for the appearance of the red-optical and near-infrared spectrum of LSR

¹Visiting Astronomer at the Infrared Telescope Facility, which is operated by the University of Hawai‘i under cooperative Agreement no. NCC 5-538 with the National Aeronautics and Space Administration, Office of Space Science, Planetary Astronomy Program.

²Spitzer Fellow

1610–0040. Although we are unable to definitively classify LSR 1610–0040, the preponderance of evidence suggests that it is a mildly metal-poor M dwarf. Finally, we tentatively identify a new band of TiO at $\sim 0.93 \mu\text{m}$ in the spectra of M dwarfs.

Subject headings: infrared: stars — stars: late-type — stars: low-mass, brown dwarfs — subdwarfs: individual (LHS 3409, LHS 1135, LSR 2036+5059) — stars: individual (LSR 1610–0040)

1. Introduction

In recent years a large population of objects with masses at and below the hydrogen burning minimum mass of $\sim 0.075 M_{\odot}$ (HBMM; Burrows et al. 2001) has been discovered (e.g., Kirkpatrick et al. 1999; Phan-Bao et al. 2001; Knapp et al. 2004). The majority of these objects were identified in wide-field surveys such as the Two Micron All Sky Survey (2MASS; Skrutskie et al. 1997), the Deep Near Infrared Southern Sky Survey (DENIS; Epchtein et al. 1997), and the Sloan Digital Sky Survey (SDSS; York et al. 2000). These “ultracool” dwarfs represent an extension of the near-solar-metallicity M dwarfs (which dominate the stellar population in the solar neighborhood in both number and mass) to lower masses and thus cooler effective temperatures. Indeed the creation of two new spectral classes, ‘L’ and ‘T’, was required in order to properly classify these objects.

Despite the enormous increase in the number of catalogued ultracool dwarfs, only a limited number of ultracool *subdwarfs* are known. Late-type (FGKM) subdwarfs are metal-poor stars that lie to the left of the main sequence in the Hertzsprung-Russell (H-R) diagram (Sandage & Eggen 1959). The position of these subdwarfs in the H-R diagram is a consequence of their reduced atmospheric opacity, which results in effective temperatures that are higher than those of their equivalent-mass main sequence counterparts. Since these stars are typically members of the halo population, they have high space motions relative to the Sun and therefore are usually identified as high proper-motion objects (e.g., Luyten 1979). Due to the intrinsic faintness of M subdwarfs and their paucity in the solar neighborhood, only a few late-type M subdwarfs are known and as a result, current spectral classification schemes are limited to spectral types earlier than sdM7 (Gizis 1997). Nevertheless, ~ 10 subdwarfs with spectral types that appear to be later than sdM7, including two L subdwarfs, have recently been discovered with 2MASS (Burgasser et al. 2003; Burgasser 2004) and in new optical proper motion surveys (Pokorny et al. 2004; Lépine & Shara 2005).

The first L-type subdwarf, 2MASS 0532+8246 (hereafter 2MASS 0532), was discovered

serendipitously by Burgasser et al. (2003) in a search for T dwarfs in the 2MASS database. Its spectrum exhibits Rb I and Cs I lines, pressure-broadened Na I and K I lines, and FeH and CrH bands in the red optical, and H₂O bands in the near infrared, all of which are consistent with an L-type dwarf. However it also exhibits CaH absorption, the deepest 0.986 μm FeH bandhead of any late-type dwarf known, and collision-induced H₂ 1–0 quadrupole absorption (CIA H₂) centered at 2.4 μm (Borysow 2002) which heavily suppresses the flux in the *H* and *K* bands (Saumon et al. 1994; Leggett et al. 2000). Enhanced hydride bands and strong H₂ absorption are indications of a metal-depleted, high-pressure atmosphere (Bessell 1982; Saumon et al. 1994; Allard & Hauschildt 1995). This, along with its high proper motion ($\mu=2''.60 \text{ yr}^{-1}$) and radial velocity ($v_{\text{rad}}=-195 \text{ km s}^{-1}$), led Burgasser et al. (2003) to classify 2MASS 0532 as an L-type subdwarf (sdL).

A second candidate L-type subdwarf, LSR 1610–0040 (hereafter LSR 1610), was discovered soon after by Lépine et al. (2003a) in a search of the Digitized Sky Survey for high proper motion stars (Lépine et al. 2002). Its red-optical spectrum is atypical, exhibiting absorption features found in the spectra of both late-type dwarfs and subdwarfs. Even though the red-optical spectrum of LSR 1610 does not fit into any standard dwarf or subdwarf sequence, it clearly exhibits spectral signatures consistent with having a very cool and metal-poor atmosphere and therefore Lépine et al. (2003a) classified this object as an early-type L subdwarf.

Given the contradictory nature of the features in the red-optical spectrum of LSR 1610, and the fact that the near-infrared wavelength range is a powerful diagnostic of the gross metallicity of late-type dwarfs (e.g., CIA H₂, weak or absent CO), we have obtained a moderate resolution, 0.8–4.1 μm spectrum of LSR 1610 to re-examine the question of its spectral classification. For comparison purposes, we have also obtained 0.8–2.4 μm spectra of LHS 3409 (sdM4.5), LHS 1135 (sdM6.5), and LSR 2036+5059 (sdM7.5; Lépine et al. 2003b). In addition, our previous work (Cushing et al. 2005) provides an infrared spectral sequence of field M and L dwarfs obtained with the same instrument against which the spectrum of LSR 1610 can also be compared. We discuss the observations and data reduction in §2 while in §3, we describe the red-optical and near-infrared spectrum of LSR 1610. Finally in §4, we discuss several possible explanations for the appearance of the spectrum of LSR 1610.

2. Observations and Data Reduction

Our observations were conducted with SpeX (Rayner et al. 2003), the facility near-infrared medium-resolution cross-dispersed spectrograph at the 3.0 m NASA Infrared Telescope Facility on Mauna Kea. A log of the observations, including the UT date of the

observations, spectroscopic mode, resolving power, total on-source integration time, and associated telluric standard stars, is given in Table 1. Each target was observed in the short-wavelength cross-dispersed mode (SXD; 0.8–2.4 μm) with a 0''.3-wide slit which yielded a resolving power of $R \equiv \lambda/\Delta\lambda \approx 2000$ in six spectral orders. LSR 1610 was also observed in the long-wavelength cross-dispersed mode (LXD1.9; 1.9–4.1 μm) with a 0''.8-wide slit ($R \approx 940$). The observations consisted of a series of exposures taken at two different positions along the 15''-long slit. An A0 V star was observed before or after each target to correct for absorption due to the Earth’s atmosphere and to flux calibrate the science object spectra. The airmass difference between each object and its associated “telluric standard” was always less than 0.05. Finally, a set of internal flat field and arc exposures was taken after each object/standard pair for flat fielding and wavelength calibration purposes.

The data were reduced using Spextool (Cushing et al. 2004), the IDL-based data reduction package for SpeX. The package performs nonlinearity corrections, flat fielding, optimal spectral extraction, and wavelength calibration. The spectra were corrected for telluric absorption and flux calibrated ($\pm 10\%$) using the extracted A0 V telluric standard and the technique described by Vacca et al. (2003). The spectra from the individual orders were then spliced together and the SXD and LXD1.9 spectra for LSR 1610 were combined. In order to confirm that the order merging process did not introduce any errors in the relative flux density levels of the spectra, we have computed synthetic $J - H$ and $H - K_s$ 2MASS colors for the objects using the technique described in Cushing et al. (2005). We find that the synthetic colors of the spectra agree with the published 2MASS colors¹ within the errors except for LHS 3409 whose synthetic $J - H$ color is 1.4σ redder than the 2MASS color. Finally, the published red-optical (0.6–1.0 μm) spectrum of LSR 1610 (S. Lépine 2004, private communication) was combined with the SpeX spectrum resulting in a final spectrum covering from 0.6 to 4.1 μm . We find that the overall slope of the SpeX spectrum from 0.8 to 1.0 μm is shallower than that of the optical spectrum over the same wavelength range. This discrepancy may be due to the fact that the standard stars used to calibrate the raw optical spectrum of LSR 1610 lack spectrophotometry between 8900 and 9700 \AA due to H_2O telluric absorption (Massey & Gronwall 1990).

The 0.8–2.4 μm spectra of LSR 1610 and the three M subdwarfs are shown in Figure 1. The signal-to-noise ratio (S/N) of the SXD spectra ranged from 50 up to 200 while the S/N of the LXD1.9 spectrum of LSR 1610 was ~ 50 . We do not show the 2.4–4.1 μm spectrum of LSR 1610 because it is relatively featureless. Absorption features commonly found in the spectra of late-type dwarfs and subdwarfs are indicated, including broad H_2O absorption

¹The 2MASS magnitudes were obtained from <http://cdsweb.u-strasbg.fr/viz-bin/VizieR?-source=II/246>.

bands centered at 1.4 and 1.8 μm , the Wing-Ford band of FeH at 0.986 μm and strong Na I and K I lines in the J band (e.g., Leggett et al. 2000; Burgasser 2004). Additional absorption features can also be discerned, including an Al I doublet at \sim 1.313 μm , a Ca I multiplet at \sim 2 μm , a Na I doublet at \sim 2.2 μm , overtone CO bands at \sim 2.29 μm , a K I line at 1.5167 μm , an Al I doublet at 1.6735 μm , and an FeH bandhead at 1.624 μm .

We have computed the bolometric flux of the LSR 1610 using the technique described in Cushing et al. (2005). Briefly, the 0.6–4.1 μm LSR 1610 spectrum was absolutely flux calibrated using 2MASS J -, H -, and K_s -band photometry (Lépine et al. 2003a). We then linearly interpolated from zero flux at zero wavelength to the flux density of the spectrum at 0.6 μm . The gaps in the observed spectrum were removed by linearly interpolating from the gap edges and a Rayleigh-Jeans tail was assumed for $\lambda > 4.1 \mu\text{m}$. Integrating over the spectrum yields $f_{\text{bol}} = 2.72 \pm 0.06 \times 10^{-14} \text{ W m}^{-2}$ ($m_{\text{bol}} = 14.92 \pm 0.03$)². We made no attempt to compute the bolometric fluxes of the M subdwarfs because the spectra cover only from 0.8 to 2.4 μm .

3. The Spectrum of LSR 1610–0040

3.1. The Red-Optical Spectrum

Lépine et al. (2003a) classified LSR 1610 as an early-type L subdwarf based primarily on three lines of evidence drawn from its red-optical spectrum. Firstly, the spectrum exhibits features present in L dwarf spectra including Rb I lines, a CrH bandhead, and a FeH bandhead. Secondly, the spectrum contains features indicative of a metal-poor atmosphere including strong CaH absorption, weak TiO bandheads, and weak VO absorption. Finally, the spectrum of LSR 1610 is significantly redder than the late-type M subdwarf, LSR 1425+7102 (sdM8; hereafter LSR 1425; Lépine et al. 2003c) which indicates that its spectral type is later than sdM8. Interestingly, Lépine et al. (2003a) derive a spectral type of sdM6 using the CaH2, CaH3, and TiO5 spectral indices developed by Gizis (1997) that measure the strengths of CaH and TiO bands near 7000 Å.

Figure 2 shows the 0.6–0.9 μm spectrum of LSR 1610 (Lépine et al. 2003a). Also shown for comparison purposes are the spectra of a late-type M dwarf, Gl 406 (M6 V; Kirkpatrick et al. 1991; Cushing et al. 2005), and a late-type M subdwarf LSR 1425 (Lépine et al. 2003c). The spectrum of LSR 1425 is clearly a better overall match to that of LSR 1610 than the spectrum of Gl 406. In particular, the TiO bandheads at 6569, 7589, 8432, and 8859 Å, which

² $m_{\text{bol}} = -2.5 \times \log(f_{\text{bol}}) - 18.988$ assuming $L_{\odot} = 3.86 \times 10^{26} \text{ W}$ and $M_{\text{bol}\odot} = +4.74$.

are quite prominent in the spectrum of Gl 406, are weak or absent in the spectra of LSR 1425 and LSR 1610. Due to the loss of the overlying TiO opacity, the resonance K I doublet (7665, 7699 Å), which is only weakly detected in the spectrum of Gl 406, is also prominent in the spectra of LSR 1425 and LSR 1610. Finally the spectra of both LSR 1425 and LSR 1610 exhibit strong CaH absorption from 6750 to 7050 Å. All of these features suggest LSR 1610 is a subdwarf. Despite the good agreement between the red-optical spectra of LSR 1425 and LSR 1610, the spectrum of LSR 1610 also exhibits features that are usually associated with L dwarfs including a resonant Rb I doublet (7800, 7948 Å) and CrH (8611 Å) and FeH (8692 Å) bandheads (Kirkpatrick et al. 1999). Nevertheless, Scholz et al. (2004) have shown that the spectrum of SSSPM J1444–2019, a candidate L subdwarf, also exhibits these features which suggests their presence may not be uncommon in the spectra of late-type subdwarfs. In summary, the red-optical spectrum of LSR 1610 is more similar to the spectrum of the M subdwarf LSR 1425 than to the M dwarf Gl 406.

3.2. The Near-Infrared Spectrum

Based on the properties of the red-optical spectrum, we would expect the near-infrared spectrum of LSR 1610 to exhibit features similar to those of other late-type M and L subdwarfs. Figure 3 shows the 0.9–2.4 μm spectra of LSR 1610, along with the spectrum of Gl 406 (M6 V; Cushing et al. 2005), LSR 2036 (sdM7.5), and the SpeX SXD spectrum of 2MASS 1626+3925 (hereafter 2MASS 1626, Burgasser 2004), an early-type L subdwarf. Figures 1 and 3 clearly show that LSR 1610 does not fit neatly into the M/L subdwarf sequence. Instead, we find that it exhibits a mix of characteristics found in the spectra of both M dwarfs and M subdwarfs.

As shown in Figure 3, the near-infrared spectrum of the M dwarf Gl 406 is actually a better match to that of LSR 1610 than either the spectrum of LSR 2036 or 2MASS 1626. In fact, of all the M dwarfs in the Cushing et al. (2005) sample, Gl 406 provides the best overall match to the 0.6–4.1 μm spectrum of LSR 1610. In particular, the spectrum of LSR 1610 and Gl 406 both peak at \sim 1.1 μm while the spectra of the subdwarfs do so shortward of \sim 1 μm . In addition, the spectra of Gl 406 and LSR 1610 both exhibit overtone CO bandheads and a Na I doublet in the *K* band, and a K I line and FeH bandhead in the *H* band. All of these features are either absent or weak in the spectra of late-type M and L subdwarfs which, taken at face value, suggests that LSR 1610 is an M dwarf. Finally, Burgasser (2004) found that the K I doublet lines in the *J*-band spectra of 2MASS 1626 and 2MASS 0532 are \sim 20% broader than in the spectra of field L dwarfs of similar spectra types (Kelu-1AB (L2) and DENIS 0205–1159AB (L7), respectively). This effect is presumably due to pressure

broadening since the reduced metal abundances of subdwarfs allows observations of deeper, and thus higher pressure, layers of the atmosphere. We measured the FWHM of the short-wavelength K I doublet in the spectrum of LSR 1610 to be 8.47 and 9.83 Å, 30–35% smaller than the values measured for the same doublet in the spectrum of Kelu-1AB (Cushing et al. 2005). This provides further evidence that LSR 1610 is not an L subdwarf. These FWHM values are, however, consistent with those measured for Gl 406 (M6 V) and are 25–30% larger than those measured for LSR 2036 (sdM7.5).

Despite the fact that the near-infrared spectrum of LSR 1610 looks superficially like an M dwarf, it also exhibits features seen in the spectra of M subdwarfs. As can be seen in Figure 3, the spectrum of LSR 1610 appears flattened relative to that of Gl 406 in the *H* and *K* bands, though not as much as 2MASS 1626. The relative flux density levels of the two spectra agree at both longer and shorter wavelengths which indicates an additional opacity source at the *H* and *K* bands may be present in the atmosphere of LSR 1610. The most obvious candidate is collision-induced H₂ absorption centered at 2.4 μm (Borysow 2002) which suppresses the flux in the *H*- and *K*-band spectra of low-metallicity dwarfs (Saumon et al. 1994; Leggett et al. 2000). However since CIA H₂ lacks any distinct spectral features, this identification remains uncertain. As shown in Figure 4, the spectra of LSR 1610 and LSR 2036 lack the 0–0 band of the *A* $^4\Pi$ – *X* $^4\Sigma^-$ transition of VO centered at ∼1.06 μm which is prominent in the spectra of late-type M dwarfs (Cushing et al. 2005). The absence of this band is consistent with the weak VO bands seen in the red-optical spectrum of LSR 1610. Finally, the lines composing the *a* 5F – *z* $^5F^\circ$ Ti I multiplet centered at 0.97 μm are stronger in the spectrum of LSR 1610 than in typical M dwarfs (e.g., Gl 406); the line strengths are more consistent with those in the spectra of M subdwarfs (e.g., LSR 2036).

Since the spectrum of LSR 1610 exhibits features found in both M dwarf and M subdwarf spectra, and does not match the spectral energy distribution of known L dwarfs and L subdwarfs, it is clear that based on its gross near-infrared properties, LSR 1610 has a spectral type of M rather than L. To further constrain its spectral type, we have computed the equivalent widths (EWs) of the short wavelength K I doublet (1.169/1.177 μm) following the technique described in Cushing et al. (2005) for LSR 1610 and the M subdwarfs in our sample. We have also computed the McLean et al. (2003) CO and *z*-FeH flux ratios that measure the strengths of the 2.29 μm CO bandhead and the 0.986 μm FeH bandhead, respectively. The results are given in Table 2. Figure 5 shows the K I EWs and CO and *z*-FeH flux ratios of LSR 1610 and the M subdwarfs as a function of spectral type. Also shown are the values for the M dwarfs in the Cushing et al. sample. If we assume LSR 1610 is a dwarf, the EWs of the K I lines and the spectral ratios indicate LSR 1610 has a spectral type of M5–M7 V, in agreement with the spectral type of ∼M6 V estimated from the overall spectral energy distribution of LSR 1610. We note, however, that the EWs of

the K I lines and the strength of the FeH bandhead are also consistent with LSR 1610 being an M subdwarf with a spectral type later than sdM7.5. Furthermore, the strength of the CO bandhead is also consistent with LSR 1610 being an M subdwarf with a spectral type of \sim sdM6.

Finally there are also two features in the spectrum that are inconsistent with our tentative classification of LSR 1610 as an M dwarf/subdwarf. The first is the strength of the Al I lines. As can be seen in Figure 4, the doublet at $1.313\text{ }\mu\text{m}$ is much stronger in the spectrum of LSR 1610 than in either the spectrum of Gl 406 or LSR 2036. We have computed the EW of this doublet for LSR 1610 and the M subdwarfs in our sample and the results are given in Table 2. The EW of the doublet in the spectrum of LSR 1610 is a factor of ~ 3 greater than that measured for the three M subdwarfs and typical M dwarfs (Cushing et al. 2005). We also note that the Al I doublet is absent in the spectra of L dwarfs (McLean et al. 2003; Cushing et al. 2005) and L subdwarfs (Burgasser 2004). Additional Al I lines at $1.1259\text{ }\mu\text{m}$ (see Figure 4) and $1.674\text{ }\mu\text{m}$ are also present in the spectrum of LSR 1610. These lines are detected only in the spectra of M dwarfs with spectral types earlier than M5 V (Cushing et al. 2005) and in only one of the three M subdwarfs in our sample (LHS 3409, sdM4.5).

The second feature is an unidentified, triangular-shaped, absorption band centered at $0.9375\text{ }\mu\text{m}$ and extending from 0.927 to $0.950\text{ }\mu\text{m}$. As can be seen in Figure 4, the spectrum of LSR 2036 lacks an absorption band at this wavelength while the spectrum of Gl 406 exhibits a broader, more bowl-shaped absorption feature centered at $0.933\text{ }\mu\text{m}$ and extending from 0.920 to $0.952\text{ }\mu\text{m}$. We have compared the spectrum of LSR 1610 to the absorption cross-section spectra of a number of species with bands near $0.9375\text{ }\mu\text{m}$ including TiO, TiH, H₂O, and VO in attempt to determine the carrier of the unidentified band. The cross-section spectra were kindly provided by R. Freedman (2005, private communication) and were computed at $T=2000\text{ K}$ and $P=1\text{ bar}$. None of these species has a band that matches the position, depth, or shape of the band in the spectrum of LSR 1610. In the appendix, we show that the absorption band at $0.933\text{ }\mu\text{m}$ in the spectra of M dwarfs is carried, at least in part, by TiO. In particular, the absorption from 0.920 to $0.927\text{ }\mu\text{m}$ can be entirely accounted for by TiO. The lack of absorption at these wavelengths in the spectrum of LSR 1610 is consistent with the weak TiO bands seen in the red-optical spectrum.

4. Discussion and Conclusions

Table 3 summarizes the spectral features identified in the spectrum of LSR 1610 along with the best estimate of the spectral type of LSR 1610 obtained from each feature. The red-optical spectrum clearly suggests an M subdwarf spectral type while the near-infrared

spectrum suggests an M dwarf spectral type. It therefore seems that the spectrum of LSR 1610 does not fit into either the tentative M/L subdwarf sequence or the well-established M/L dwarf sequence.

What then to make of LSR 1610? There are a number of possibilities that might explain the contradictory spectral features.

M Dwarf with Low Oxygen Abundance— If we posit that LSR 1610 is an M dwarf with an overall metallicity near solar, then the features most at odds with this classification are the weak TiO and VO bands in the red-optical. The weakness of these bands and the strengths of the Ti I lines at $\sim 0.97 \mu\text{m}$ could simultaneously be explained by assuming a low oxygen abundance relative to solar; the abundance of TiO and VO would decrease due to the loss of O and the relative abundance of the gas-phase Ti would consequently increase (Lodders 2002). However the strengths of the H₂O and CO bands in the near-infrared are not atypical for M dwarfs/subdwarfs and thus eliminate this possibility.

M Dwarf with Enhanced Grain Formation— The TiO and VO bands weaken across the M→L dwarf transition (Jones & Tsuji 1997; Kirkpatrick et al. 1999) due, in part, to the formation of titanium- and vanadium-bearing condensates (Burrows & Sharp 1999; Lodders 2002). The M→L transition occurs at $T_{\text{eff}} \simeq 2300 \text{ K}$ (Golimowski et al. 2004) while LSR 1610 has $T_{\text{eff}} \simeq 2700 \text{ K}$ if we assume it has a spectral type of M6 V (see §3.2). This indicates that any condensation would have to be significantly enhanced. The presence and strength of the Ti I, Ca I, Mg I, and Al I lines in the spectrum of LSR 1610 belie this hypothesis since we would expect that these refractory elements would also be removed from the atmosphere by condensation (Burrows & Sharp 1999; Lodders 2002).

Peculiar M Subdwarf— LSR 1610 could be a peculiar M subdwarf. In this case, then the presence of the Na I doublet and CO overtone bands in the *K* band, and the K I line, FeH bandhead, and Al I doublet in the *H* band must be explained. One possibility is that these species are overabundant. However the strengths of Na I and K I lines in the *J* band and the FeH bandhead at $0.986 \mu\text{m}$ are not anomalous. An alternative hypothesis is that the collision-induced H₂ absorption in the *H* and *K* bands is unusually weak allowing these features to emerge. Since the strength of the CIA H₂ is sensitive to the atmospheric pressure, and the atmospheric pressure is, all else being equal, proportional to the surface gravity of the object, this may indicate LSR 1610 has a low surface gravity. However the *H* and *K* band spectrum of LSR 1610 appears flatter than the spectrum of LSR 2036 (sdM7.5) which argues against this hypothesis.

M/L Dwarf Binary— Since LSR 1610 exhibits features seen in the spectra of M and L dwarfs, could it be an unresolved M/L binary? We find this hypothesis unlikely for

three reasons. Firstly, L dwarfs are fainter than M dwarfs at both optical and near-infrared wavelengths which would make the detection of the Rb I lines and FeH and CrH bandheads in a composite M/L spectrum unlikely. Secondly, the optical spectrum of LSR 1610 lacks the 8521 Å Cs I line, which is a distinctive feature in the spectra of L dwarfs (Kirkpatrick et al. 1999). Finally, the overall red-optical spectrum of LSR 1610 is completely inconsistent with that of M and L dwarfs (Kirkpatrick et al. 1999).

Mildly Metal-Poor M Dwarf— The overall spectral energy distribution of LSR 1610 is clearly best matched by that of Gl 406, an M6 dwarf. If we therefore assume that LSR 1610 is a mid-type M dwarf, we can explain many of the seemingly disparate spectral features if we further posit that it is mildly metal poor. A metallicity intermediate between M dwarfs and M subdwarfs would explain the subdwarf-like spectral features (weak TiO and VO bands, mild CIA H₂, and prominent Ti I lines) and the dwarf-like spectral features (CO bands, Na I doublet, 1.617 μ m FeH bandhead, and 1.516 μ m K I line). Given the information currently available for LSR 1610, we find this to be the most plausible explanation for the features seen in its spectrum.

Nevertheless, none of the above scenarios can explain the strengths of the Al I lines in the spectrum of LSR 1610 and in particular, the anomalously large EW of the Al I doublet at 1.313 μ m. Since the strength of the H₂O absorption that provides the continuum at this wavelength appears normal, we conclude Al I must be overabundant relative to solar. In addition, there remains the unidentified molecular absorption band centered at 0.9375 μ m that is completely inconsistent with the spectra of known M dwarfs and M subdwarfs. Since the parallax of LSR 1610 has yet to be measured, it is difficult to further constrain its nature. It is, however, currently being observed as part of the United States Naval Observatory (USNO) faint star parallax program (H. Harris 2005, private communication). The forthcoming parallax measurement can then be combined with our f_{bol} measurement (see §2) to compute its bolometric luminosity which may shed further light on the nature of LSR 1610.

The authors wish to thank S. Lépine for providing the optical spectrum of LSR 1610–0040, A. Burgasser for providing the spectrum of 2MASS 1626+3925, R. Freedman for providing the molecular cross-section data, A. Burgasser and J. Liebert for stimulating discussions, and the anonymous referee whose suggestions improved the paper. This publication makes use of data from the Two Micron All Sky Survey, which is a joint project of the University of Massachusetts and the Infrared Processing and Analysis Center, and funded by the National Aeronautics and Space Administration and the National Science Foundation. This research has made use of the SIMBAD database, operated at CDS, Strasbourg, France and NASA’s Astrophysics Data System Bibliographic Services. M.C.C. acknowledges financial support

from the NASA Infrared Telescope Facility and NASA through the Spitzer Space Telescope Fellowship Program.

A. The Tentative Identification of a New TiO Band in M Dwarf Spectra

In the course of attempting to identify the absorption band at $0.9375 \mu\text{m}$ in the spectrum of LSR 1610, we found that the identification of H_2O as the primary carrier of an absorption band centered at $\sim 0.933 \mu\text{m}$ in the spectra of M dwarfs by Cushing et al. (2005) was in error. That identification was based on the apparent coincidence between the position of the absorption band in the spectra of M dwarfs and the telluric H_2O band. In this appendix, we show that this band is carried, at least in part, by TiO.

Figure 6 shows the $R \approx 2000$ spectrum of a typical late-type M dwarf vB 10 (M8 V; Cushing et al. 2005) in the upper panel and the cross-section data of TiO and H_2O in the middle and lower panels, respectively. The spectrum of vB 10 has a $\text{S}/\text{N} > 100$. The cross-section data, which were computed at $T=2000 \text{ K}$ and $P=1 \text{ bar}$ (R. Freedman 2005, private communication), have been smoothed to $R=2000$ and resampled onto the wavelength grid of vB 10. The absorption band, which covers from 0.92 to $\sim 0.948 \mu\text{m}$, is clearly inconsistent with the H_2O cross-section spectrum. However the TiO data matches the width of the band relatively well.

The absorption band actually appears to have two distinct parts, ranging from 0.92 to $0.927 \mu\text{m}$ and 0.927 to $0.948 \mu\text{m}$. The 0.92 to $0.948 \mu\text{m}$ section of the band can be accounted for by TiO but the rest of the band is probably carried by a combination of TiO, H_2O and some as-yet unidentified species. Indeed there appears to be additional bandheads at 0.9370 , 0.9416 , and $0.9441 \mu\text{m}$ that are absent in the TiO or H_2O data. Higher resolution spectra will be required to both confirm the identification of TiO as a partial carrier of this band and identify any additional carriers.

REFERENCES

Allard, F. & Hauschildt, P. H. 1995, *ApJ*, 445, 433

Bessell, M. S. 1982, *Proceedings of the Astronomical Society of Australia*, 4, 417

Borysow, A. 2002, *A&A*, 390, 779

Burgasser, A. J. 2004, *ApJ*, 614, L73

Burgasser, A. J., Kirkpatrick, J. D., Burrows, A., Liebert, J., Reid, I. N., Gizis, J. E., McGovern, M. R., Prato, L., & McLean, I. S. 2003, *ApJ*, 592, 1186

Burrows, A., Hubbard, W. B., Lunine, J. I., & Liebert, J. 2001, *Reviews of Modern Physics*, 73, 719

Burrows, A. & Sharp, C. M. 1999, *ApJ*, 512, 843

Cushing, M. C., Rayner, J. T., & Vacca, W. D. 2005, *ApJ*, 623, 1115

Cushing, M. C., Vacca, W. D., & Rayner, J. T. 2004, *PASP*, 116, 362

Epcstein, N., de Batz, B., Capoani, L., Chevallier, L., Copet, E., Fouque, P., Lacombe, F., Le Bertre, T., Pau, S., Rouan, D., Ruphy, S., Simon, G., Tiphene, D., Burton, W. B., Bertin, E., Deul, E., Habing, H., Borsenberger, J., Dennefeld, M., Guglielmo, F., Loup, C., Mamon, G., Ng, Y., Omont, A., Provost, L., Renault, J.-C., Tanguy, F., Kimeswenger, S., Kienel, C., Garzon, F., Persi, P., Ferrari-Toniolo, M., Robin, A., Paturel, G., Vauglin, I., Forveille, T., Delfosse, X., Hron, J., Schultheis, M., Appenzeller, I., Wagner, S., Balazs, L., Holl, A., Lepine, J., Boscolo, P., Picazzio, E., Duc, P.-A., & Mennessier, M.-O. 1997, *The Messenger*, 87, 27

Gizis, J. E. 1997, *AJ*, 113, 806

Gizis, J. E. & Reid, I. N. 1997, *PASP*, 109, 849

Golimowski, D. A., Leggett, S. K., Marley, M. S., Fan, X., Geballe, T. R., Knapp, G. R., Vrba, F. J., Henden, A. A., Luginbuhl, C. B., Guetter, H. H., Munn, J. A., Canzian, B., Zheng, W., Tsvetanov, Z. I., Chiu, K., Glazebrook, K., Hoversten, E. A., Schneider, D. P., & Brinkmann, J. 2004, *AJ*, 127, 3516

Jones, H. R. A. & Tsuji, T. 1997, *ApJ*, 480, L39

Kirkpatrick, J. D., Henry, T. J., & McCarthy, D. W. 1991, *ApJS*, 77, 417

Kirkpatrick, J. D., Reid, I. N., Liebert, J., Cutri, R. M., Nelson, B., Beichman, C. A., Dahn, C. C., Monet, D. G., Gizis, J. E., & Skrutskie, M. F. 1999, *ApJ*, 519, 802

Knapp, G. R., Leggett, S. K., Fan, X., Marley, M. S., Geballe, T. R., Golimowski, D. A., Finkbeiner, D., Gunn, J. E., Hennawi, J., Ivezić, Z., Lupton, R. H., Schlegel, D. J., Strauss, M. A., Tsvetanov, Z. I., Chiu, K., Hoversten, E. A., Glazebrook, K., Zheng, W., Hendrickson, M., Williams, C. C., Uomoto, A., Vrba, F. J., Henden, A. A., Luginbuhl, C. B., Guetter, H. H., Munn, J. A., Canzian, B., Schneider, D. P., & Brinkmann, J. 2004, *AJ*, 127, 3553

Leggett, S. K., Allard, F., Dahn, C., Hauschildt, P. H., Kerr, T. H., & Rayner, J. 2000, *ApJ*, 535, 965

Lépine, S., Rich, R. M., & Shara, M. M. 2003a, *ApJ*, 591, L49

—. 2003b, *AJ*, 125, 1598

Lépine, S. & Shara, M. M. 2005, *AJ*, 129, 1483

Lépine, S., Shara, M. M., & Rich, R. M. 2002, *AJ*, 124, 1190

—. 2003c, *ApJ*, 585, L69

Lodders, K. 2002, *ApJ*, 577, 974

Luyten, W. J. 1979, LHS catalogue. A catalogue of stars with proper motions exceeding $0.^{\circ}5$ annually (Minneapolis: University of Minnesota, 1979, 2nd ed.)

Massey, P. & Gronwall, C. 1990, *ApJ*, 358, 344

McLean, I. S., McGovern, M. R., Burgasser, A. J., Kirkpatrick, J. D., Prato, L., & Kim, S. S. 2003, *ApJ*, 596, 561

Phan-Bao, N., Guibert, J., Crifo, F., Delfosse, X., Forveille, T., Borsenberger, J., Epchtein, N., Fouqué, P., & Simon, G. 2001, *A&A*, 380, 590

Pokorny, R. S., Jones, H. R. A., Hambly, N. C., & Pinfield, D. J. 2004, *A&A*, 421, 763

Rayner, J. T., Toomey, D. W., Onaka, P. M., Denault, A. J., Stahlberger, W. E., Vacca, W. D., Cushing, M. C., & Wang, S. 2003, *PASP*, 115, 362

Sandage, A. R. & Eggen, O. J. 1959, *MNRAS*, 119, 278

Saumon, D., Bergeron, P., Lunine, J. I., Hubbard, W. B., & Burrows, A. 1994, *ApJ*, 424, 333

Scholz, R.-D., Lodieu, N., & McCaughrean, M. J. 2004, *A&A*, 428, L25

Skrutskie, M. F., Schneider, S. E., Stiening, R., Strom, S. E., Weinberg, M. D., Beichman, C., Chester, T., Cutri, R., Lonsdale, C., Elias, J., Elston, R., Capps, R., Carpenter, J., Huchra, J., Liebert, J., Monet, D., Price, S., & Seitzer, P. 1997, in *The Impact of Large Scale Near-IR Sky Surveys*, ed F. Garzón, N. Epchtein, A. Omont, W. B. Burton, & P. Persi (Dordrecht: Kluwer), 25

Vacca, W. D., Cushing, M. C., & Rayner, J. T. 2003, *PASP*, 115, 389

York, D. G., Adelman, J., Anderson, J. E., Anderson, S. F., Annis, J., Bahcall, N. A., Bakken, J. A., Barkhouser, R., Bastian, S., Berman, E., Boroski, W. N., Bracker, S., Briegel, C., Briggs, J. W., Brinkmann, J., Brunner, R., Burles, S., Carey, L., Carr, M. A., Castander, F. J., Chen, B., Colestock, P. L., Connolly, A. J., Crocker, J. H., Csabai, I., Czarapata, P. C., Davis, J. E., Doi, M., Dombeck, T., Eisenstein, D., Ellman, N., Elms, B. R., Evans, M. L., Fan, X., Federwitz, G. R., Fiselli, L., Friedman, S., Frieman, J. A., Fukugita, M., Gillespie, B., Gunn, J. E., Gurbani, V. K., de Haas, E., Haldeman, M., Harris, F. H., Hayes, J., Heckman, T. M., Hennessy, G. S., Hindsley, R. B., Holm, S., Holmgren, D. J., Huang, C., Hull, C., Husby, D., Ichikawa, S., Ichikawa, T., Ivezić, Ž., Kent, S., Kim, R. S. J., Kinney, E., Klaene, M., Kleinman, A. N., Kleinman, S., Knapp, G. R., Korienek, J., Kron, R. G., Kunszt, P. Z., Lamb, D. Q., Lee, B., Leger, R. F., Limmongkol, S., Lindenmeyer, C., Long, D. C., Loomis, C., Loveday, J., Lucinio, R., Lupton, R. H., MacKinnon, B., Mannery, E. J., Mantsch, P. M., Margon, B., McGehee, P., McKay, T. A., Meiksin, A., Merelli, A., Monet, D. G., Munn, J. A., Narayanan, V. K., Nash, T., Neilsen, E., Neswold, R., Newberg, H. J., Nichol, R. C., Nicinski, T., Nonino, M., Okada, N., Okamura, S., Ostriker, J. P., Owen, R., Pauls, A. G., Peoples, J., Peterson, R. L., Petravick, D., Pier, J. R., Pope, A., Pordes, R., Prosapio, A., Rechenmacher, R., Quinn, T. R., Richards, G. T., Richmond, M. W., Rivetta, C. H., Rockosi, C. M., Ruthmansdorfer, K., Sandford, D., Schlegel, D. J., Schneider, D. P., Sekiguchi, M., Sergey, G., Shimasaku, K., Siegmund, W. A., Smee, S., Smith, J. A., Snedden, S., Stone, R., Stoughton, C., Strauss, M. A., Stubbs, C., SubbaRao, M., Szalay, A. S., Szapudi, I., Szokoly, G. P., Thakar, A. R., Tremonti, C., Tucker, D. L., Uomoto, A., Vanden Berk, D., Vogeley, M. S., Waddell, P., Wang, S., Watanabe, M., Weinberg, D. H., Yanny, B., & Yasuda, N. 2000, AJ, 120, 1579

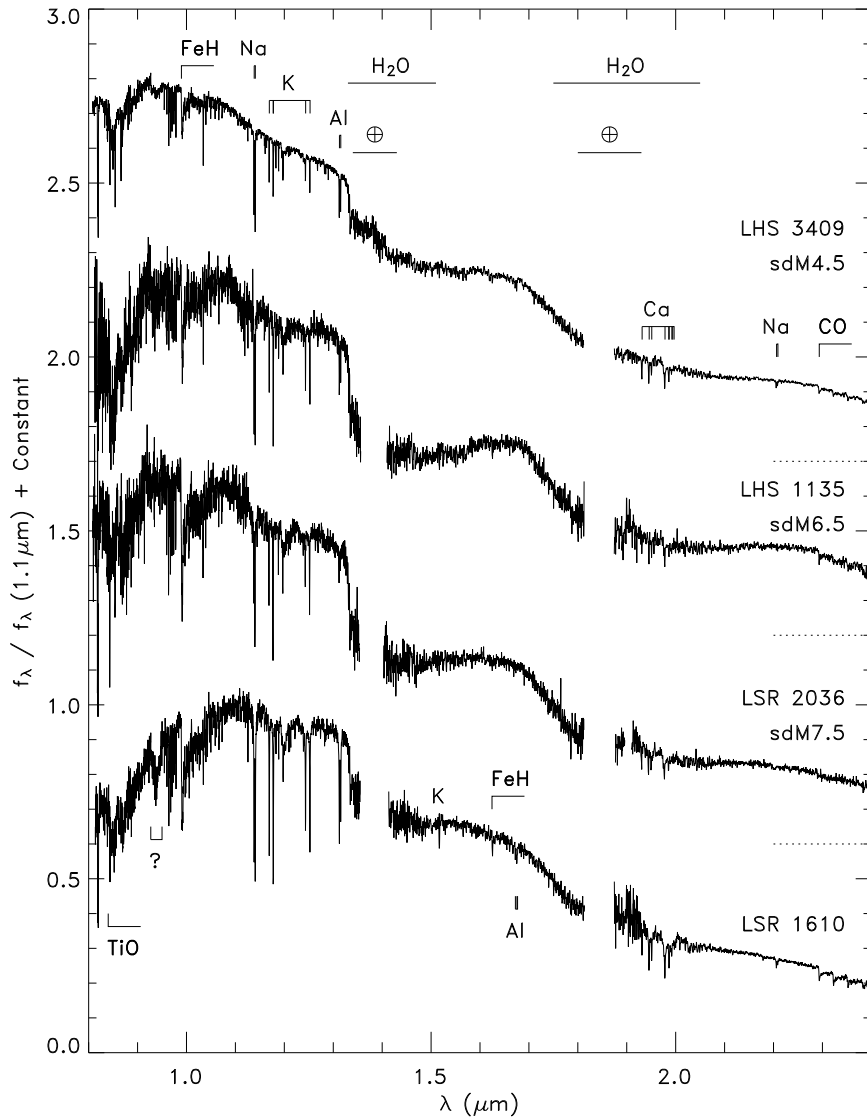


Fig. 1.— The 0.8–2.4 μm spectra of LHS 3409 (sdM4.5), LHS 1135 (sdM6.5), LSR 2036 (sdM7.5), and LSR 1610–0040. The spectra have been normalized at 1.1 μm and offset by constants (*dotted lines*). The most prominent atomic and molecular absorption features are indicated. The gap in the spectra at $\sim 1.85 \mu\text{m}$ is due to a gap in the wavelength coverage of the SXD mode of SpeX while the data were removed at 1.4 μm due to low a signal-to-noise ratio.

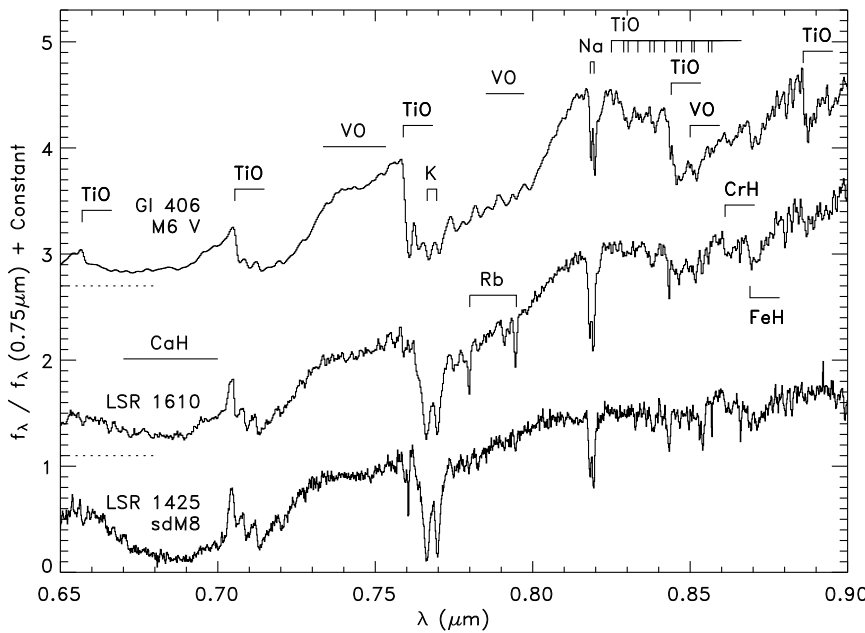


Fig. 2.— The 0.65–0.9 μm spectra of Gl 406 (M6 V; Kirkpatrick et al. 1991; Cushing et al. 2005), LSR 1610 (Lépine et al. 2003a) and LSR 1425+7102 (sdM8; Lépine et al. 2003c). The spectra have been normalized at 0.75 μm and offset by constants (*dotted lines*). The most prominent atomic and molecular absorption features are indicated.

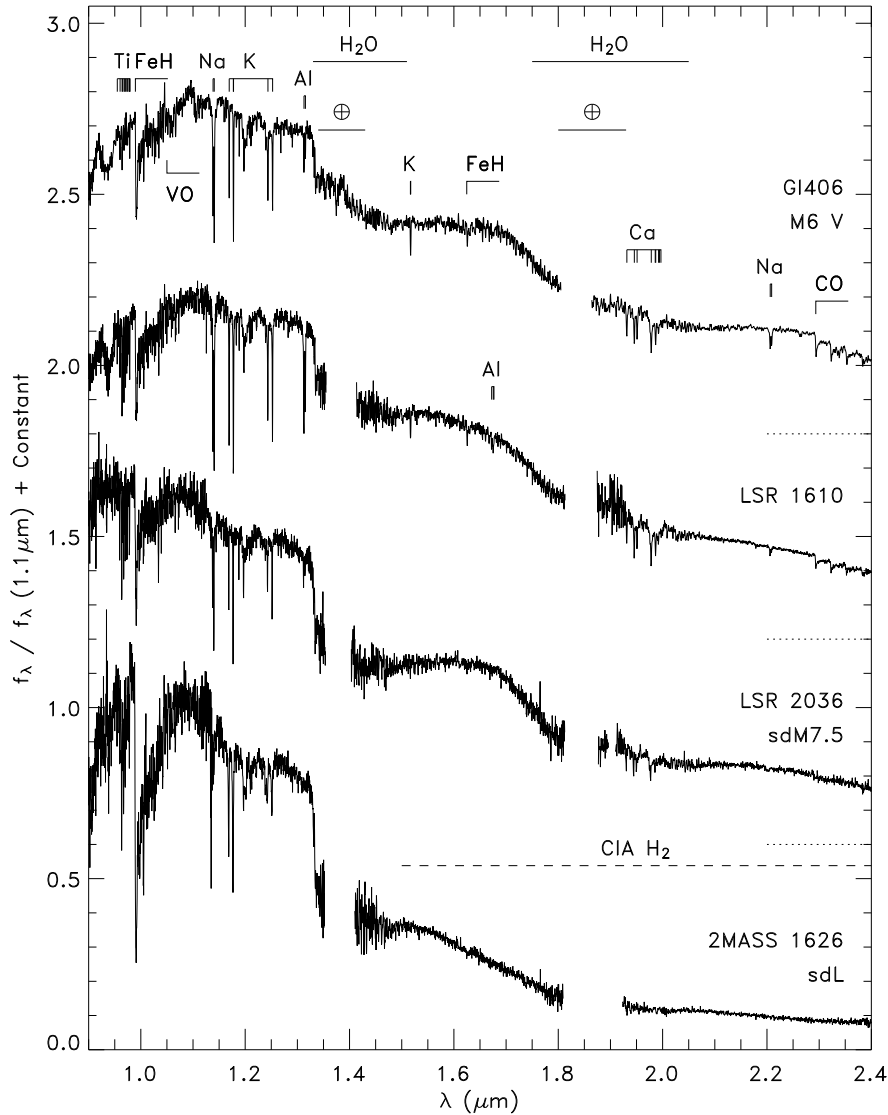


Fig. 3.— The 0.9–2.4 μm spectra of Gl 406 (M6 V; Cushing et al. 2005), LSR 1610, LSR 2036 (sdM7.5), and 2MASS 1626+3925 (Burgasser 2004). The spectra have been normalized at 1.1 μm and offset by constants (*dotted lines*). The most prominent atomic and molecular absorption features are indicated.

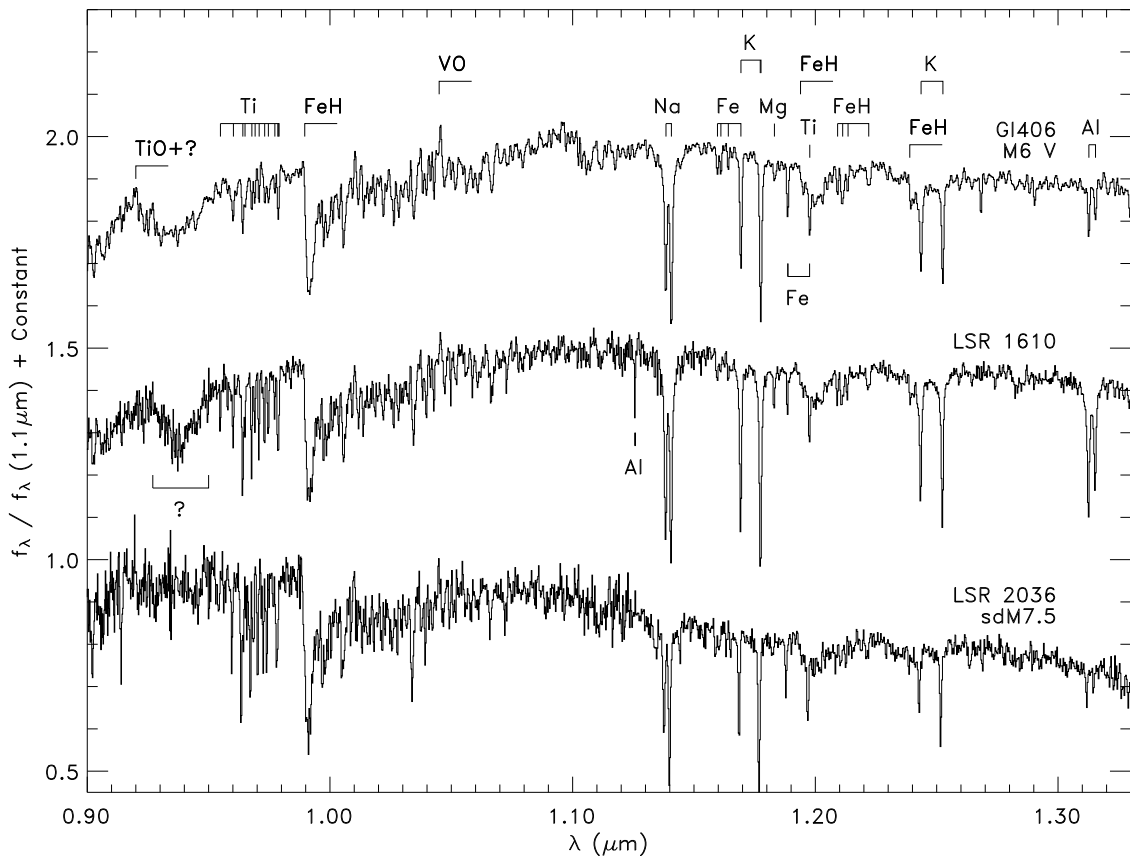


Fig. 4.— The 0.9–1.34 μm spectra of Gl 406 (M6 V; Cushing et al. 2005), LSR 1610, and LSR 2036 (sdM7.5). The spectra have been normalized at 1.1 μm and offset by constants. Prominent absorption features due to FeH, Na, K, Al, and Fe are indicated. Note the strong Al doublet at $\sim 1.315 \mu\text{m}$ and the Al I line at 1.12 μm in the spectrum of LSR 1610.

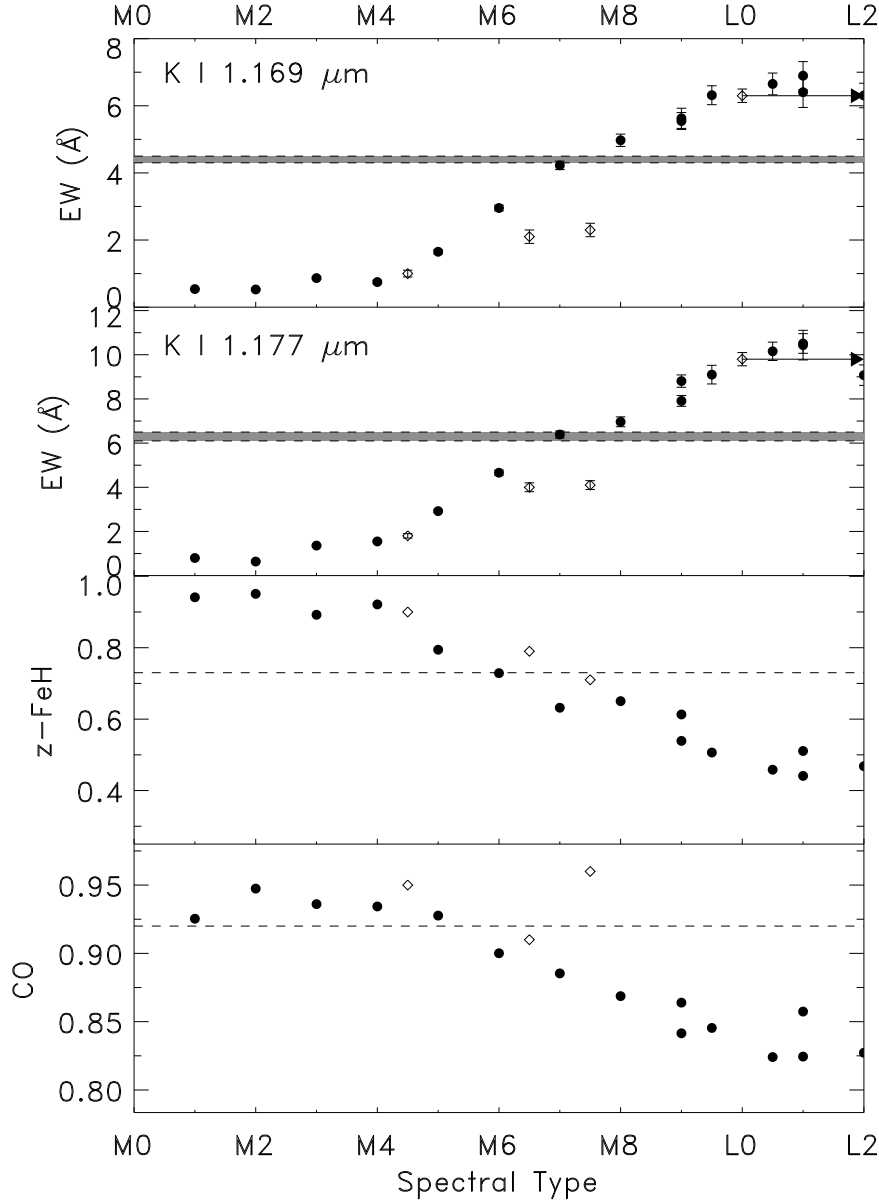


Fig. 5.— The EWs of the $1.169 \mu\text{m}$ and $1.177 \mu\text{m}$ K I lines and the CO and z -FeH flux ratios of McLean et al. (2003) as a function of spectral type. The M dwarfs from the Cushing et al. (2005) sample are shown as filled circles while the M subdwarfs in the current sample are shown as diamonds. The EW of 2MASS 1626+2925 is shown as a lower limit since its spectral subclass is unknown. The values for LSR 1610 are indicated by dashed lines; the greyed region denotes the $\pm 1\sigma$ EW range.

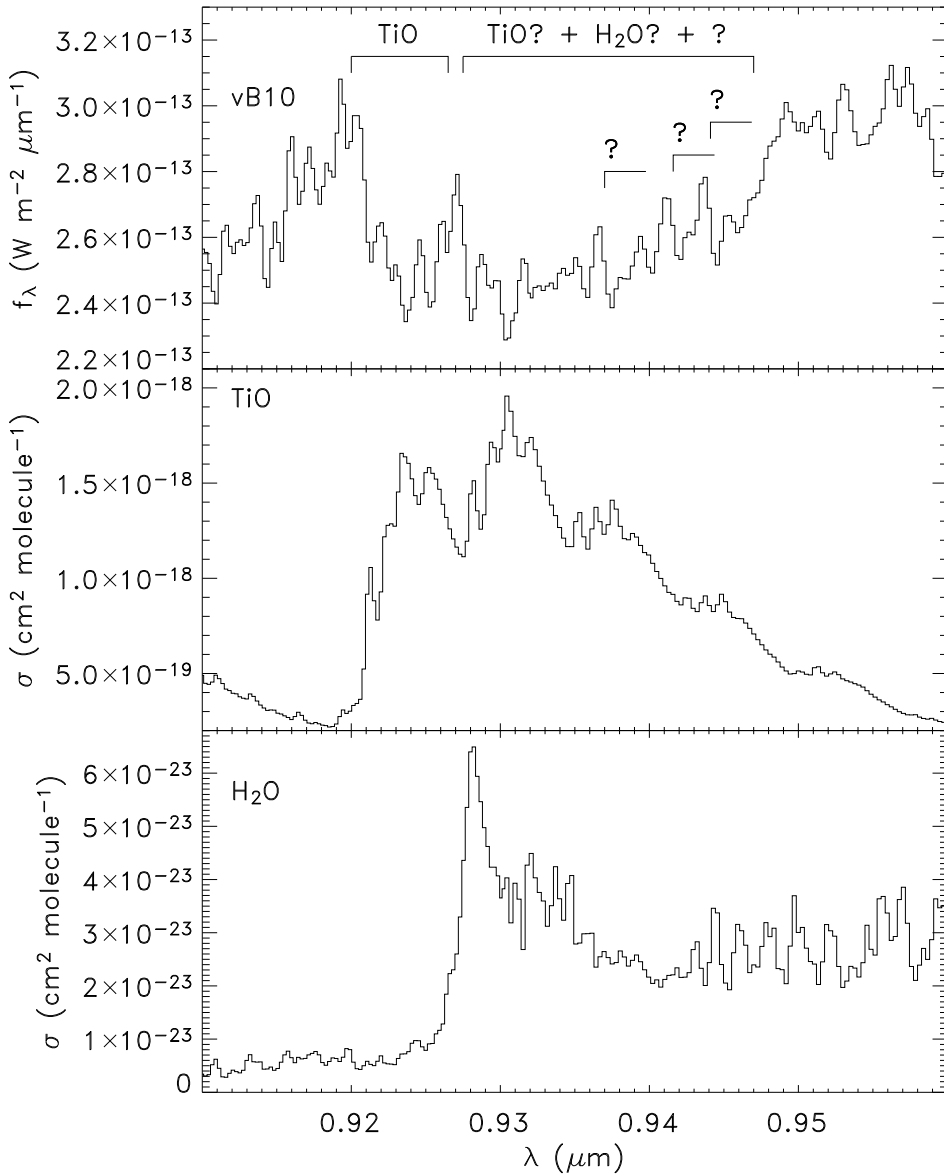


Fig. 6.— *Bottom:* Cross-section spectrum of H₂O at $T=2000$ K and $P=1$ bar. *Middle:* Cross-section spectrum of TiO at $T=2000$ K and $P=1$ bar. *Top:* Spectrum of vB 10 (M8 V; Cushing et al. 2005). The broad absorption band in the spectrum of vB 10 is carried, at least in part, by TiO.

Table 1. Log of SpeX Observations

Object	Spectral ^a Type	UT Date	Spectroscopic Mode	<i>R</i>	Exp. Time (sec)	A0 V Standard
LHS 3409	sdM4.5	2003–07–06	SXD	2000	1440	HD 178207
LHS 1135	sdM6.5	2003–10–15	SXD	2000	3000	HD 7215
LSR 2036+5059	sdM7.5	2003–10–06	SXD	2000	2400	HD 205314
LSR 1610–0040	sdL?	2003–07–06	SXD	2000	1680	HD 140775
		2003–07–06	LXD1.9	940	2400	HD 140775

^aThe spectral types are based on optical spectroscopy and are from Gizis & Reid (1997) and Lépine et al. (2003a,b).

Table 2. Equivalent Widths and Flux Ratios of LSR 1610–0040

Object (1)	Spectral Type (2)	EW (Å)			z-FeH (7)	CO (8)
		K I (1.169 μ m) (3)	K I (1.177 μ m) (4)	Al I (1.132 μ m) (5)		
LHS 3409	sdM4.5	1.0 ± 0.1	1.8 ± 0.1	2.5 ± 0.1	0.90	0.95
LHS 1135	sdM6.5	2.1 ± 0.2	4.0 ± 0.2	2.7 ± 0.2	0.79	0.91
LSR 2036+5059	sdM7.5	2.3 ± 0.2	4.1 ± 0.2	1.4 ± 0.2	0.71	0.96
LSR 1610–0040	sdL?	4.4 ± 0.1	6.3 ± 0.2	8.5 ± 0.2	0.73	0.92

Table 3. Summary of Features in the Spectrum of LSR 1610–0040

Feature	Wavelength (μm)	Notes	Corresponding Spectral Type
CaH band	0.6750–0.7050	Strongest in sdM	sdM6
TiO bandhead	0.7053	Strongest in late dM and sdM	M
VO band	0.7534–0.7734	Strongest in late dM and early dL	sdM
TiO bandhead	0.7589	Strongest in late dM and early dL	sdM
K I	0.7665, 0.7699	Seen in dM, dL and sdL	sdM
VO band	0.7851–0.7973	Strongest in late dM and early dL	sdM
Rb I	0.7800, 0.7948	Seen in dL	L
Na I	0.8183, 0.8195	Seen in dM, early dL, and sdM	...
TiO bandhead	0.8206	Strongest in late dM and early dL	sdM
TiO bandhead	0.8432	Strongest in dM and early dL	sdM
CrH bandhead	0.8611	Seen in dL and sdL	L
FeH bandhead	0.8692	Seen in dL and sdL	L
Ti I	0.96–0.98	Seen in dM. Strongest in sdM	sdM
FeH bandhead	0.9896	Seen in dM, dL, sdM, and sdL	~M6 V, ~sdM7
Al I	1.126	Seen only in early to mid dM and sdM	<M5
Na I	1.138, 1.140	Seen in dM, dL and sdM	M, L
K I	1.169, 1.178	Seen in dM and dL	~M7 V, ~sdM8
Al I	1.313	Seen in dM and sdM	...
K I	1.516	Seen in dM and dL and weakly in sdM	dM
FeH bandhead	1.62457	Seen in dM and dL and weakly in sdM	dM
Al I	1.674	Seen in early dM and sdM	dM
Ca I	~1.95	Seen in dM and sdM	M
Na I	2.207	Strongest in dM. Also seen in early sdM	M
CO bandheads	2.29	Strongest in dM and dL. Also seen in early sdM	~M5.5 V, ~sdM6

Note. — M = M dwarf or M subdwarf, dM = M dwarf, sdM = M subdwarf, L = L dwarf or L subdwarf, dL = L dwarf, sdL = L subdwarf